Effect of Tooth Profile Modification on the Durability of Planetary Hub Gears

E. Fatourehchi[1], M. Mohammadpour[1,*], P.D. King[1], H. Rahnejat[1], G. Trimmer[2], R. Womersley[2] and A. Williams[2]

[1] *Wolfson School of Mechanical, Electrical and Manufacturing Engineering, Loughborough University, LE113TU*
[2] *JCB Transmission, Wrexham Industrial Estate, Wrexham, UK*
[*]Corresponding author: m.mohammad-pour@lboro.ac.uk

Abstract:

Planetary systems offer the advantage of desired speed-torque variation with a lighter, compact and coaxial construction than the traditional gear trains. Frictional losses and Noise, Vibration and Harshness (NVH) refinement are the main concerns. Modification of gear teeth geometry to reduce friction between the mating teeth flanks of vehicular planetary hubs, as well as refining NVH under varying load-speed conditions is one of the remedial actions. However, implementing modifications can result in reduced structural integrity and system durability. Therefore, a contradiction may arise between assuring a high degree of durability and achieving better transmission efficiency, which necessitates detailed system optimisation.

An integrated multi-disciplinary analytical approach, including tribology and sub-surface stress analysis is developed. As a preliminary step, Tooth Contact Analysis (TCA) is performed to obtain contact footprint shape of meshing gear teeth pairs, as well as contact kinematics and applied load distribution. Then, an analytical time-efficient Elastohydrodynamic Lubrication (EHL) analysis of elliptical point contact of crowned spur gear tooth is carried out to observe the effect of gear tip relief modification upon planetary hub sub-surface stresses.

Keywords— Transmission system durability, Gear tooth modification, Planetary wheel hub systems

1-Introduction

A large number of mechanical applications, ranging from wind turbines to automotive powertrains use planetary gears. This is because they provide a set of transmission ratios and provide improved efficiency relative to fixed axes transmissions [1].

A number of studies have focused on the transmission efficiency of planetary gear systems [1-4]. However, in many cases improving the transmission efficiency can result in reduced structural integrity and system durability. This necessitates an in-depth stress analysis, integrated with analysis of system efficiency in order to arrive at an optimal practical solution.

Evaluation of sub-surface stress distribution in medium to high loaded contacts is important as these determine the fatigue life of machine elements. Highly loaded gear contacts are generally subjected to high sub-surface stresses. Lundberg and Palmgren [5] carried out one of the first studies in this field. They investigated fatigue mechanism in roller bearings and showed the significance of generated sub-surface stress field. They discovered that one of the critical parameters in initiating fatigue cracks in a contact is the location of maximum sub-surface shear stress. The cyclic nature of contact causes the crack to propagate and finally reach the contacting surface, leading to the formation of spalls. A comprehensive treatment of 3D sub-surface stress field for elastohydrodynamic contacts (such as gears ad bearings) was reported in [6], which showed that the reversing cyclic orthogonal shear stresses play a more poignant role in load bearing conjunctions. In elastohydrodynamic contacts the presence of the pressure spike in the vicinity of the contact outlet also sets up a localised sub-surface stress field with higher maximum shear stresses which occur closer to the contact surface as shown by Teodorescu et al [7] in the case of cam-tappet contact. This localised field can initiate premature spalling [6]. Recently Li et al. [8] developed a numerical model to predict fatigue crack formation in spur gear contacts working under mixed elastohydrodynamic regime of lubrication. The model was compared with measured gear fatigue stress-life data, showing reasonable accuracy in predicting the crack nucleation fatigue life, as well as the location of the critical failure sites. Fatourehchi et al. [9] developed a numerical model to investigate the effect of different gear teeth modifications on spur gear power loss and durability of high performance transmission systems. Nevertheless, both studies are associated with a single gear contact operating under moderate to high speeds.

With regard to planetary gears, Jao et al. [10] performed a fatigue test on an automatic transmission planetary gear which consisted of a forward sun gear, a reverse sun gear, 3 short and 3 long pinions. They observed that macro-pitting and bending fatigue are the primary causes of failure in gears. Dong et al. [11] developed a simplified model to predict the fatigue life of contacting gears of a wind turbine planetary gear sets operating under dynamic conditions. Their study showed that the pitting is more

likely to occur on the sun gear rather than the planet gears. Moreover, the recess area is the critical location in terms of pitting. This is because the equivalent contact radius within the recess area of the sun and planet gears is much smaller than at the pitch and contacting regions. Therefore, maximum contact pressure occurs in the recess area.

Bahk and Parker [12] developed an analytical model to investigate the effect of tooth profile modification on spur planetary gear vibration. Tooth profile modification can minimise vibration in certain vibration modes than others. Therefore, the most active modes need to be considered when applying optimal gear tooth profile modification in order to minimise gear vibration.

Inevitable manufacturing errors cause the applied load not to be shared equally within the different sun-planet and planet-ring meshes. This is another parameter which can be a troublesome for gear durability. Ligata et al. [13] carried out an experimental study of the effects of manufacturing errors on planetary system gear stresses. They studied the influence of the number of planets, torque levels, and the carrier pinhole positional errors. Their results indicated that increasing the number of planets makes the generated stresses more sensitive to the carrier pinhole positional error. Fatourehchi et al. [14] developed a tribo-dynamic model to investigate the effect of mesh phasing due to manufacturing errors on the planetary system efficiency and NVH refinement. The model was capable of predicting the optimal level of combined efficiency and NVH performance of a planetary system.

In this paper, a parametric analysis is conducted in order to investigate the effect of different extents of tooth profile modifications on planetary hub gears' sub-surface stresses in off-highway applications. There has been a dearth of work reported for this type of planetary hub gears for trucks and off-highway vehicles operating under high loads and low speeds. These operational conditions are critical in terms of tribology with increased contact pressures of up to 1.2 GPa and a sub-micrometre lubricant film thickness. Planetary hub systems are particularly compact, resulting in teeth pair contacts of highly concentrated nature. Fatigue spalling due to sub-surface stress field is common in practice. Thus, a numerical model capable of predicting the parameters which affect planetary hub gears' generated sub-surface stresses is the key to achieving a reliable system. The developed model provides realistic conditions with rapid cost-effective simulations. It takes into account the shear in the contacting region,

as well as the normal generated pressures for better estimation of the sub-surface stress field. This approach has not hitherto been reported in literature for planetary wheel hub gears.

2- Planetary hub configuration

The studied planetary hub gear system is shown schematically in Figure 1. The figure also shows the power flow from the gearbox through to the planetary wheel hubs. The transmission ratio, speed and torques at different transmission stages are also indicated in the figure. The sun gear is attached to the input shaft which transfers power from the differential. The ring gear is attached and fixed to the housing. The carrier transfers the output power of the planetary hub system to the wheels. The planetary system comprises three planet gears. The study assumes no misalignment in the system. It is also assumed that the input power from the sun gear is divided equally among the planets.

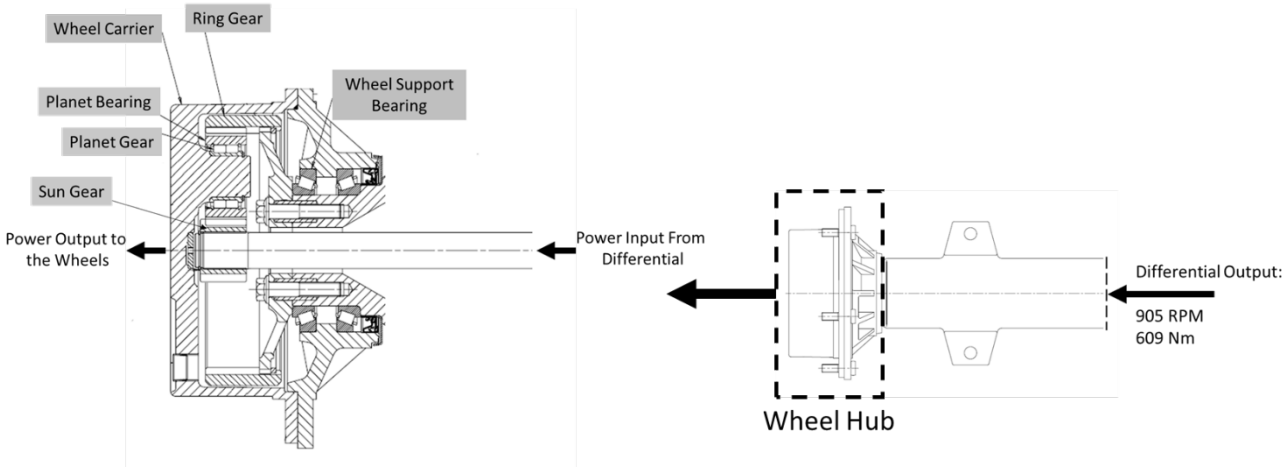

Figure 1: Schematic representation of the planetary wheel hub gears configuration and the power flow

3- Methodology

Normal generated contact pressure and tangential traction distributions over the contact patch at any location along a meshing cycle are needed in order to evaluate the generated sub-surface stress field. An integrated Tooth Contact Analysis (TCA) and an analytical elastohydrodynamic method are introduced. At any location along the meshing cycle, the instantaneous radii of curvature of the meshing teeth, as well as contact surface velocities and the orthogonal meshing contact loads are obtained through the tooth contact analysis (TCA). These parameters form the input to the analytical elastohydrodynamic analysis, yielding the normal generated pressures (assumed as Hertzian) and viscous friction (i.e. tangential traction). The methodology is based on quasi-static analysis. This is necessary to perform rapid cost-effective simulations, suitable for industrial use. Therefore, dynamics of the planetary hub system is neglected. Furthermore, this study does not take into account the effect of manufacturing errors on the planetary system durability.

3.1 – Tooth Contact Analysis

The approach of Vijayakar [15], and Xu and Kahraman [16] is utilized to develop the TCA model. The developed model obtains the instantaneous contact geometry, rolling/sliding velocity and load share per teeth pair contact [16, 17] for simultaneous meshing of sun-planet and planet-ring contacts in the planetary hub system.

3.2- Subsurface Stresses

Contacting gear surfaces transmit the generated normal pressures and tangential traction due to viscous friction. Normal pressure $p(x)$ and tangential traction $q(x)$ over the strip $(-b < x < a)$ in an elastic half-space are shown in Figure 2.

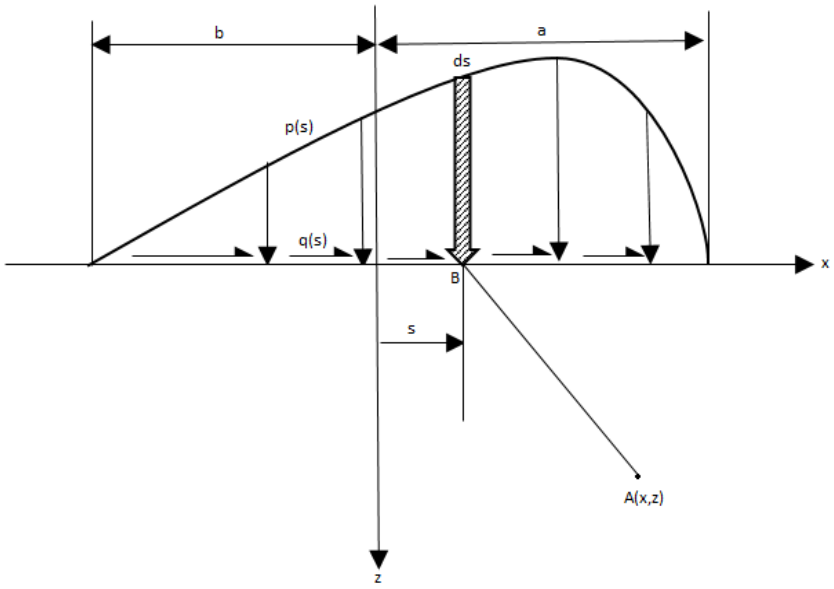

Figure 2: Normal pressure and tangential traction distribution over the solid surface (after Johnson [18])

According to Johnson [18], the sub-surface stress distribution at an arbitrary point A (Figure 2) within the body of contacting solids induced by p(x) and q(x) becomes:

$$\sigma_x = -\frac{2z}{\pi}\int_{-b}^{a}\frac{p(s)(x-s)^2 ds}{[(x-s)^2+z^2]^2} - \frac{2}{\pi}\int_{-b}^{a}\frac{q(s)(x-s)^3 ds}{[(x-s)^2+z^2]^2} \quad (1)$$

$$\sigma_z = -\frac{2z^3}{\pi}\int_{-b}^{a}\frac{p(s)ds}{[(x-s)^2+z^2]^2} - \frac{2z^2}{\pi}\int_{-b}^{a}\frac{q(s)(x-s)ds}{[(x-s)^2+z^2]^2} \quad (2)$$

$$\tau_{xz} = -\frac{2z^2}{\pi}\int_{-b}^{a}\frac{p(s)(x-s)ds}{[(x-s)^2+z^2]^2} - \frac{2z}{\pi}\int_{-b}^{a}\frac{q(s)(x-s)^2 ds}{[(x-s)^2+z^2]^2} \quad (3)$$

The elastohydrodynamic model is developed to obtain the tangential traction due to viscous friction, q(x). The proposed analytical model is time-efficient, simulating a meshing cycle of a spur gear pair in a couple of seconds. This is essential in performing a parametric study of the effect of gear tip relief modification upon planetary hub generated sub-surface stress field. The contact pressure is obtained based on Hertzian theory (which closely agrees with the prevailing elastohydrdynamic conditions, particularly for the usually starved transmission gearing). Therefore, the usually generated EHL pressure spike at the vicinity of the contact outlet is neglected. The method is explained in the next section.

According to the Hertzian theory:

$$p(x) = \frac{2W}{\pi a^2}(a^2 - x^2)^{1/2} \quad (4)$$

where:

$$a^2 = \frac{4WR}{\pi E_r} \quad (5)$$

The maximum pressure is:

$$p_0 = \left(\frac{WE_r}{\pi R}\right)^{1/2} \quad (6)$$

The key points with regard to the structural integrity of the mating gear teeth surfaces is the choice of yielding criterion for inelastic deformation. The general consensus for bearing and gear surfaces is the cyclic repetitive nature of orthogonal shear stresses, given by equation (3). These occur in depths closer to the contacting surface with a larger double amplitude (cyclic tensile-compressive). The cyclic nature of gear contact causes the bulk material to be sheared in one direction and then in the opposite sense. The alternating shear stress field, τ_{zx} occur in pairs at 90° to each other in the auxiliary planes [6]. The equivalent stress, σ_e with the alternating shear stress hypothesis is [19]:

$$\sigma_e = 2|\tau_{zxmaz}| \quad (7)$$

where the double amplitude for σ_e remains approximately the same with any additional surface traction [20]. The onset of yielding according to the alternating shear stress hypothesis is when the equivalent stress reaches half the yield stress of the material (i.e. structural integrity is assured, when: σ_e<1/2 σ_y).

3.3 – The elastohydrodynamic model

High contact pressures of up to 1.2 GPa, in the planetary wheel hub system of trucks and off-highway applications can result in high pressure viscous shear in the contact. Mixed regime of lubrication is also expected due to very thin lubricant films. Tangential traction in the contact is obtained as:

$$q = \frac{(f_v + f_b)}{A} \quad (8)$$

where, f_v is the viscous friction and f_b is the boundary friction in the contact, and A is the apparent contact area.

3.3.1 – Viscous friction

Evans and Johnson [21] developed an analytical method to determine viscous friction in elastohydrodynamic contacts, where the coefficient of friction is obtained as:

$$\mu = \frac{f_v}{W} = 0.87\alpha\tau_0 + 1.74\frac{\tau_0}{\bar{p}} ln\left[\frac{1.2}{\tau_0 h_{c0}}\left(\frac{2K^*\eta_0}{1+9.6\xi}\right)^{\frac{1}{2}}\right] \quad (9)$$

where, W is the normal contact load, obtained from the TCA model, and ξ is:

$$\xi = \frac{4}{\pi}\frac{K}{h_{c0}/R}\left(\frac{\bar{p}}{E'RK'\rho'c'U_r}\right)^{1/2} \quad (10)$$

Chittenden et al. [22] equation is used to calculate the thin lubricant film thickness under the instantaneous operating conditions which is required for equation (10).

$$h_{c0}^* = 4.31U_e^{0.68}G_e^{0.49}W_e^{-0.073}\left\{1 - exp\left[-1.23\left(\frac{R_y}{R_x}\right)^{2/3}\right]\right\} \quad (11)$$

where, the dimensionless groups are expressed as:

$$U_e = \frac{\pi\eta_0 U}{4E_r R_x}, W_e = \frac{\pi W}{2E_r R_x^2}, G_e = \frac{2}{\pi}(E_r\alpha), h_{c0}^* = \frac{h_0}{R_x}$$

Table 1 lists the lubricant properties.

Table 1: Lubricant properties

Pressure viscosity coefficient (Pa^{-1})	2.38×10^{-8}
Lubricant Atmospheric dynamic viscosity at 100°C (Pa.s)	0.0144
Ambient value of lubricant limiting shear stress (MPa)	2
Thermal conductivity of fluid (W/mK)	0.140
Pressure-induced shear coefficient (ε)	0.047

3.3.2 – Boundary Friction

The high contact pressures of planetary gear systems result in thin lubricant films of the order of surface roughness. Therefore, some degree of interaction of asperities on the counter face contacting surfaces occurs. These interactions promote boundary friction. In this study, Greenwood and Tripp [23] method is utilized in predicting boundary friction. When the Stribeck's oil film parameter falls within the range: $1 < \lambda = \frac{h_{c0}}{\sigma} < 2.5$, mixed regime of lubrication occurs. Under these conditions, the share of contact load which is carried by the contact of asperity heights is:

$$W_a = \frac{16\sqrt{2}}{15}\pi(\xi\beta\sigma)^2\sqrt{\frac{\sigma}{\beta}}E'AF_{5/2}(\lambda) \tag{12}$$

where, the statistical function $F_{5/2}(\lambda)$, assuming a Gaussian distribution of asperities is obtained as [24]:

$$F_{5/2} = \begin{cases} -0.004\lambda^5 + 0.057\lambda^4 - 0.29\lambda^3 + 0.784\lambda^2 - 0.784\lambda + 0.617 & \text{for } \lambda < 2.5 \\ 0; & \text{for } \lambda \geq 2.5 \end{cases} \tag{13}$$

The roughness parameter ($\xi\beta\sigma$) for steel surfaces is generally in the range 0.03–0.07 [23]. Average asperity slope [20], σ/β, is usually in the range of 10^{-4}-10^{-2}. In the current study, these parameters were obtained through measurement of a typical gear tooth topography as: $\xi\beta\sigma = 0.055$ and $\sigma/\beta = 10^{-3}$ [25].

A thin film of boundary active lubricant additives (a tribo-film) is usually adsorbed or bonded to the summit of the contacting asperities or is entrapped in their inter-spatial valleys. This lubricant film is subjected to non-Newtonian shear, thus:

$$f_b = \tau_L A_a \tag{14}$$

where τ_L is the lubricant's limiting shear stress:

$$\tau_L = \tau_0 + \varepsilon^* P_m \tag{15}$$

where, the mean pressure P_m is obtained as:

$$P_m = \frac{W_a}{A_a} \tag{16}$$

The asperity contact area is [23]:

$$A_a = \pi^2(\xi\beta\sigma)^2 A F_2(\lambda) \tag{17}$$

The statistical function $F_2(\lambda)$ is obtained as [24, 25]:

$$F_2(\lambda) = \begin{cases} -0.002\lambda^5 + 0.028\lambda^4 - 0.173\lambda^3 + 0.526\lambda^2 - 0.804\lambda + 0.500 & for\ \lambda < 2.5 \\ 0; & for\ \lambda \geq 2.5 \end{cases} \tag{18}$$

4- Results and discussion

High impact loads and sharp rises in the contact pressures are more likely to occur for gear pairs with no tip relief. Under these conditions, gear teeth tip relief through removal of material ensures smoother gradual changes in profile. Applying tip relief in involute teeth can also relieve impact loads as teeth pairs come into contact. To achieve the optimum tip relief, its extent in length and amount should be determined. Figure 3 is a schematic representation of tip relief modification, showing both its amount and length.

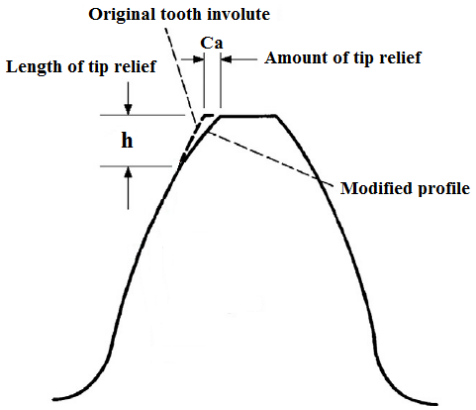

Figure 3: Schematic representation of tip relief modification

The planetary wheel hub gears of the JCB Max-Trac rear differential is investigated here. The input torque to the sun gear from the differential is 609 Nm at the speed of 906 rpm. The gear data are listed in Table 2.

Table 2: The gearbox data

Radius of sun gear	26 mm
Radius of planet gear	43 mm
Radius of ring gear	115 mm
Number of teeth for sun gear	15
Number of teeth for planet gear	25
Number of teeth for ring gear	66
Pressure angle	20°
Helix angle	0°

Two parameters are involved in the tip relief modification. These are the amount of tip relief and the length of the relieved region. Firstly, the effect of gear teeth tip relief amount is considered. Secondly, the influence of gear teeth tip relief length is investigated.

It should be noted that the results are plotted against the angular position along the path of meshing contact progression. The effect of variation of tip relief amount and tip relief length on the length of line of action is negligible and therefore, different characteristics of contact are plotted against the non-dimensional "position along the meshing cycle". It varies between 0 to 1, where "0" refers to the angular position at the onset of meshing and "1" refers to angular position at the end of a meshing cycle.

4.1- Effects of tip relief amount

The amount of tip relief (specified as C_a in figure 3) is changed from 25% to 150% of the current baseline design in order to investigate the effect of tip relief amount on the generated sub-surface stresses. Tip amounts of relief for different scenarios are listed in Table 3.

Figure 4 shows the effect of change in tip relief amount on the contact parameters (i.e. radii of curvature, rolling velocity and normal load) for a meshing cycle for both the sun-planet and the planet-ring contacts.

Table 3: Amount of tip relief for different scenarios

	Tip relief amount [%]		
Scenario	Sun	Planet	Ring
1	150	150	150
2	125	125	125
3(Current-Design)	100	100	100
4	75	75	75
5	50	50	50
6	25	25	25

	Sun-Planet Contact	Planet-Ring Contact
Radii of curvature [mm]	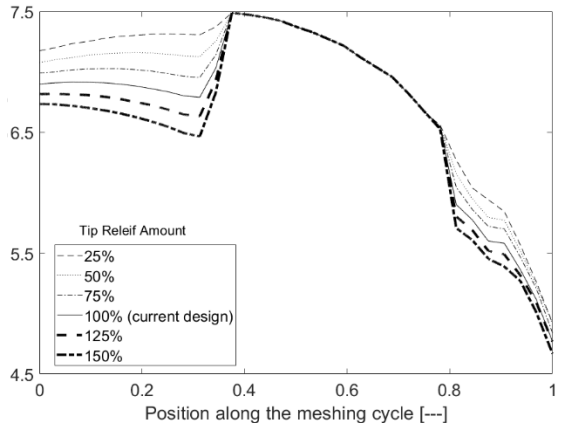	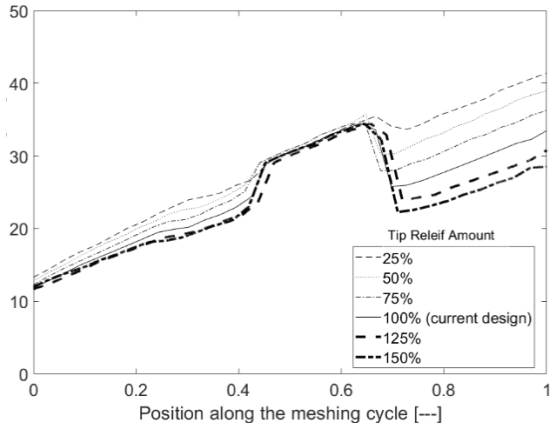
Rolling velocity [m/s]	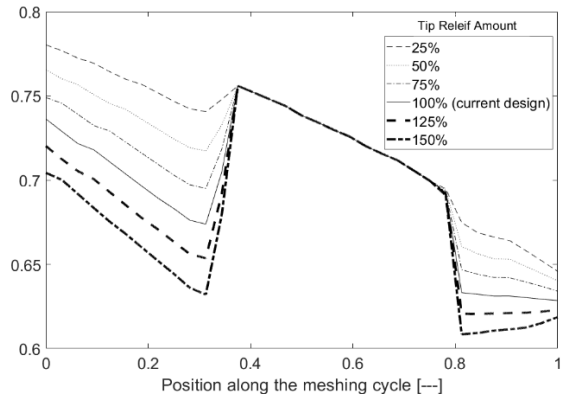	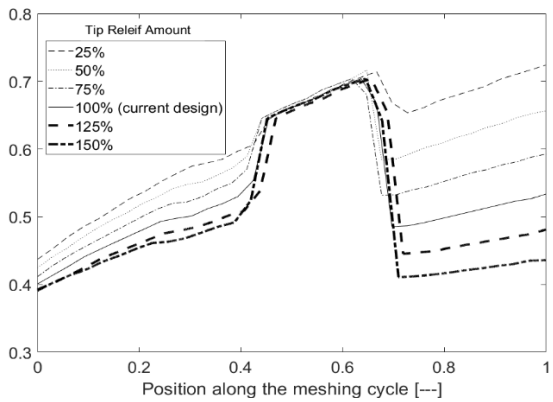

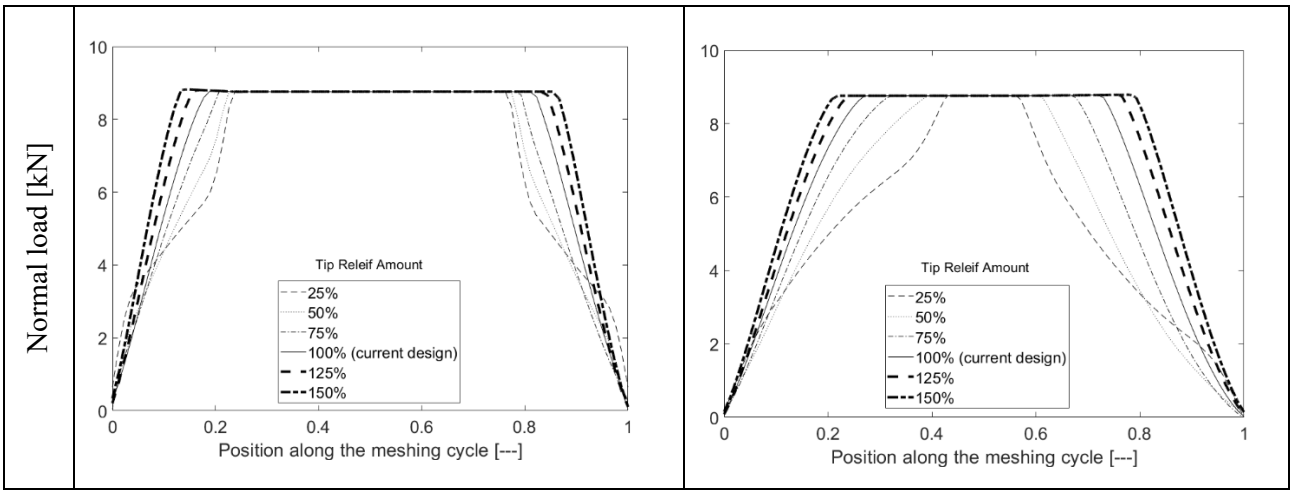

Figure 4: Contact parameters for Sun-Planet and Planet-Ring Contacts along the meshing cycle for different tip relief amounts

Figure 4 shows that increasing the amount of tip relief increases the shift in the radii of curvature and the rolling/sliding velocity at the affected region. The sudden shift is due to the use of actual coordinate information created by a simulation of the cutting process which is embedded in the utilized TCA model [26]. Moreover, this increases the duration of single contact over a meshing cycle.

According to the alternating shear stress hypothesis [6, 19], Figures 5 and 6 illustrate the variation of maximum double shear stress magnitude along the meshing cycle for different applied tip relieves for the Planet-Ring and the Sun-Planet contacts respectively.

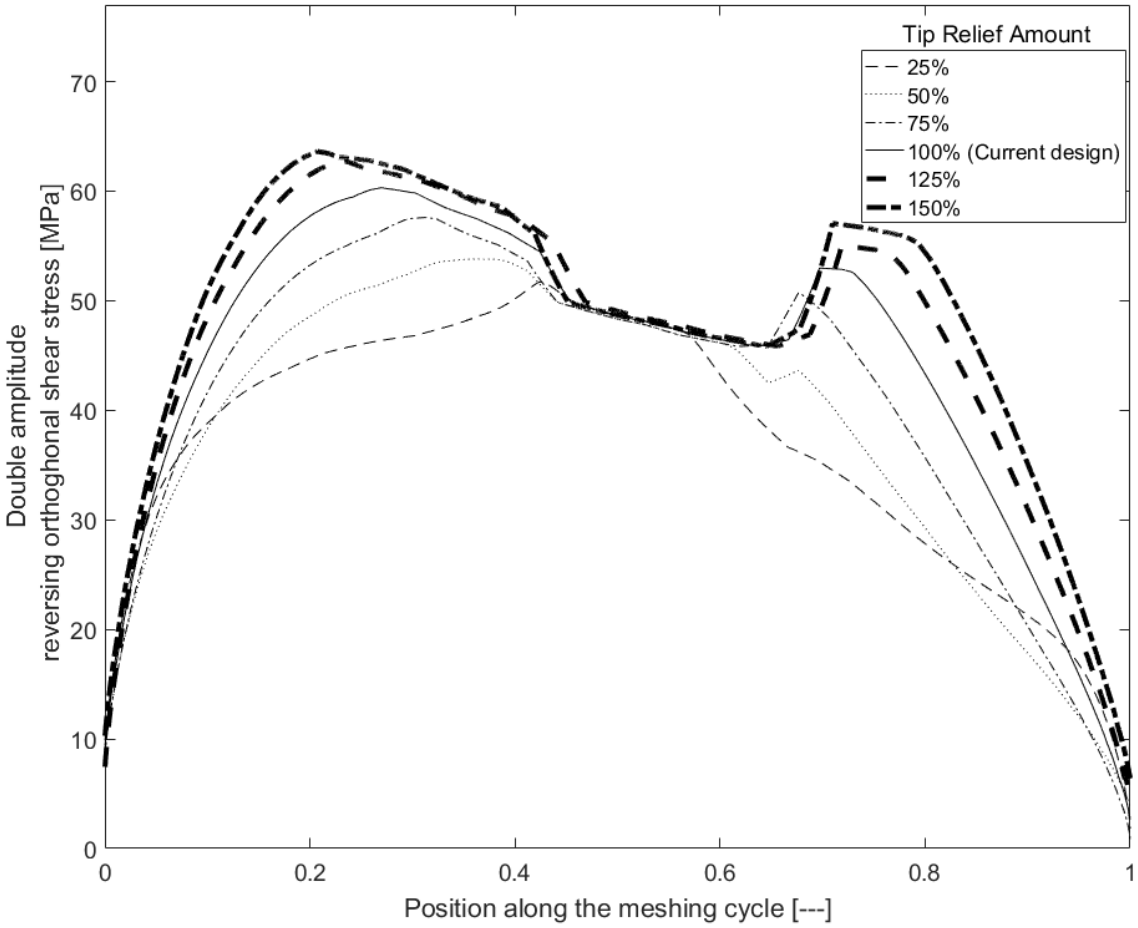

Figure 5: Double amplitude reversing orthogonal shear stress along the meshing cycle for different amounts of tip relief; Planet-Ring Contact

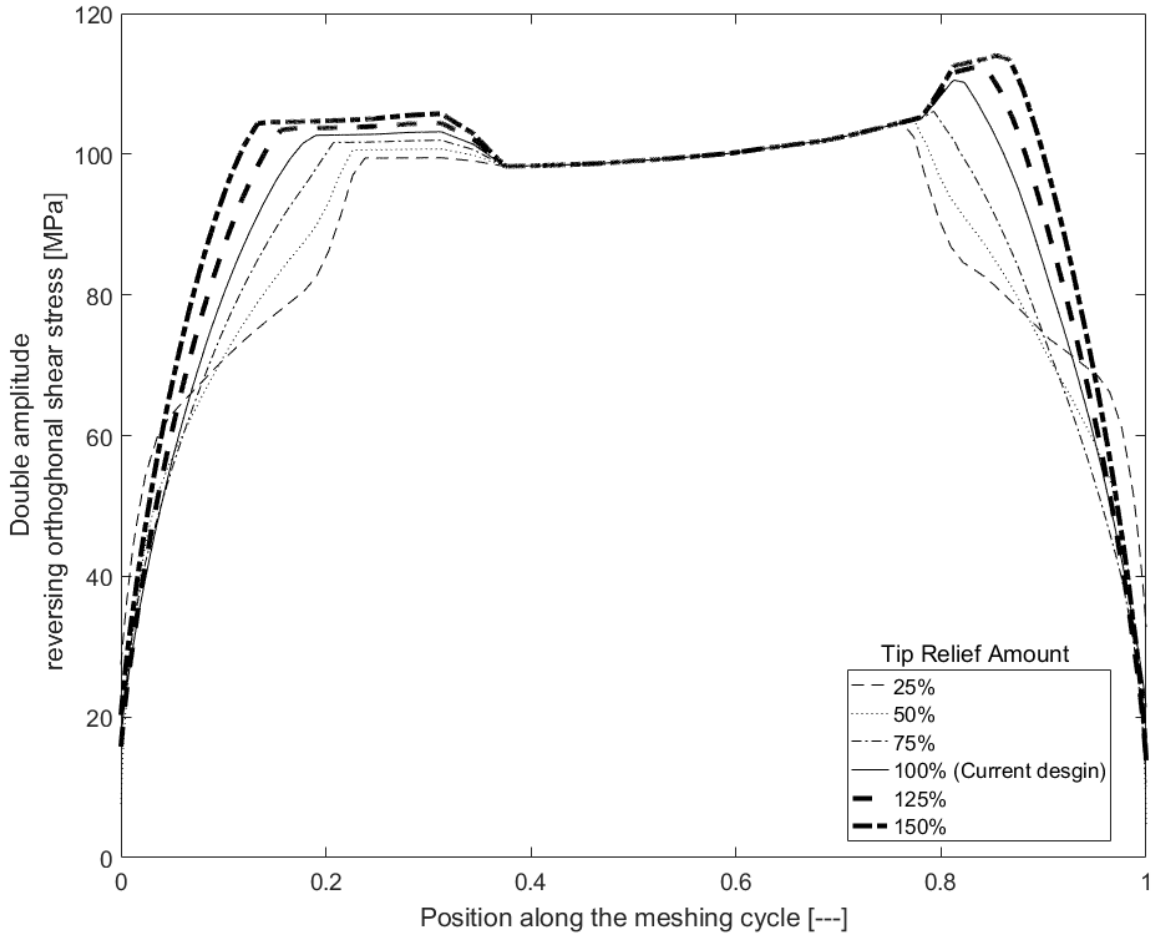

Figure 6: Double amplitude reversing orthogonal shear stress along the meshing cycle for different amounts of tip relief; Sun-Planet Contact

The tooth hardened steel yield stress is 470 MPa. Therefore, based on the shear stress criterion described in the section 3.2, the double amplitude of the alternating shear stress (i.e. the equivalent stress) should not exceed 235 MPa. According to the Figures 5 and 6, the equivalent stress remains below this limit for both Planet-Ring and Sun-Planet contacts. Increasing the amount of tip relief, the effect of alternating shear stresses becomes more pronounced. One should note that in this study, only the sub-surface shear stress field is considered as the measure for durability. Therefore, other durability parameters such as scuffing and scratching as well as NVH refinement and efficiency should also be taken into account.

Furthermore, the maximum amount of the equivalent stress in Sun-Planet contact is almost 50 MPa higher than that for the Planet-Ring contact, which indicates the fatigue failure is more likely to occur in the sun-planet contact which is in agreement with the findings in [10].

4.2- Effect of tip relief length

In order to investigate the effect of tip relief length (specified as *h* in Figure 3) on induced sub-surface stresses, the relief length is reduced from the current design (baseline value) by up to 35%. Table 4 shows the changes in the tip relief length for different scenarios.

Table 4: Length of tip relief for different scenarios

Scenario	Length of tip relief [%]		
	Sun	Planet	Ring
1(Current-Design)	100	100	100
2	75	75	75
3	50	50	50
4	37.5	37.5	37.5
5	35	35	35

Figure 7 shows the effect of change in the tip relief length on the contact parameters (i.e. radii of curvature, rolling velocity and normal load) for a meshing cycle for both the sun-planet and the planet-ring contacts.

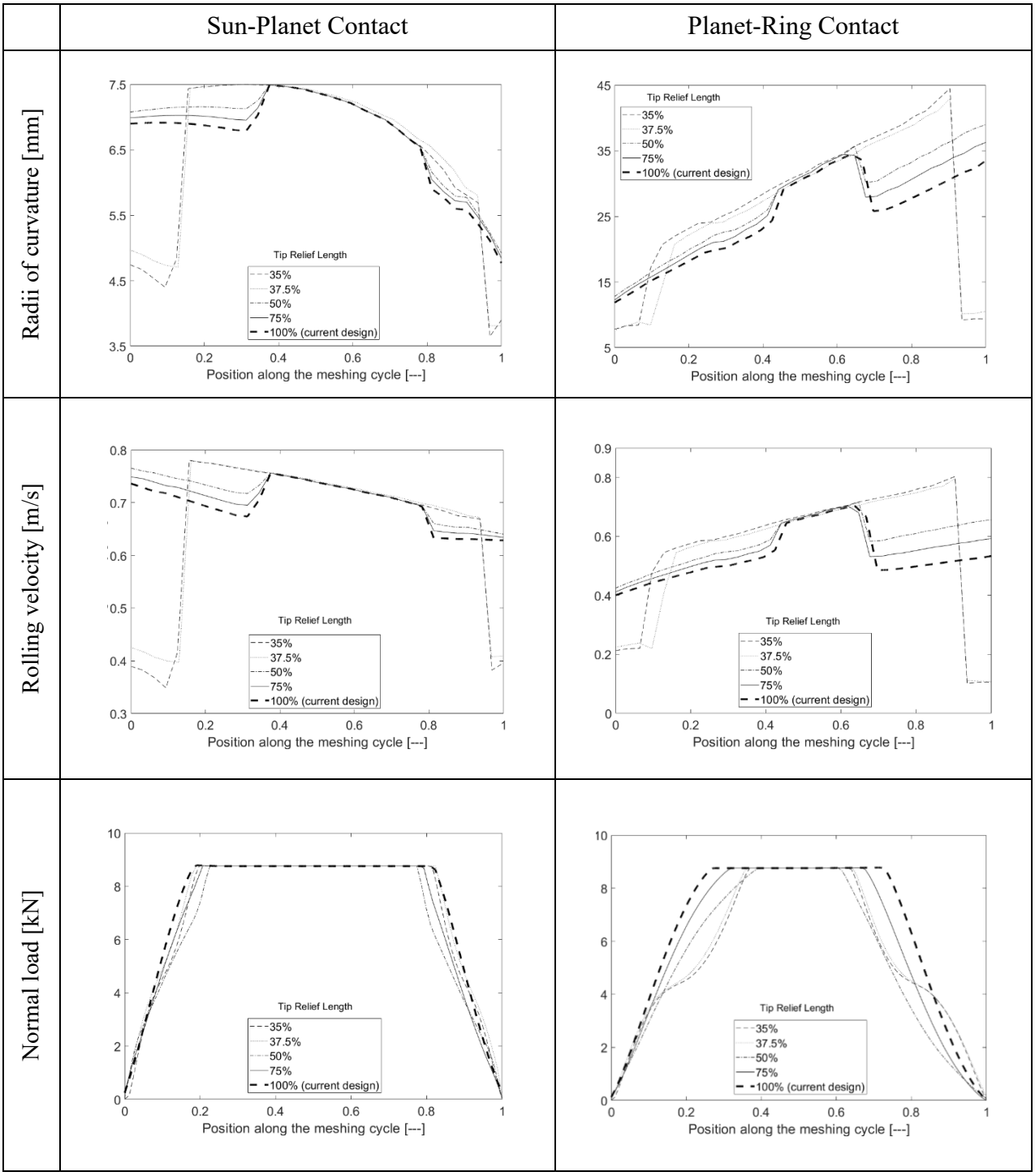

Figure 7: Contact parameters for Sun-Planet and Planet-Ring Contacts along the meshing cycle for different tip relief lengths

Figure 7 shows that changes in the tip relief length, slightly decrease the radii of curvature and rolling velocity at the affected region in cases with over 50% change. Decreasing the length of tip relief by lower amounts (i.e. studied cases of 37.5% and 35%) causes a sudden change in the radii of curvature and the corresponding contact rolling velocity. Increasing the tip relief length slightly increases the duration of a single contact over a meshing cycle, where it is more pronounced in the case of planet-ring gear contact.

Using the alternating shear stress hypothesis [6, 19], Figures 8 and 9 illustrate the variation of double amplitude reversing orthogonal shear stress along the meshing cycle for different applied tip relief lengths for the Planet-Ring and Sun-Planet contacts respectively.

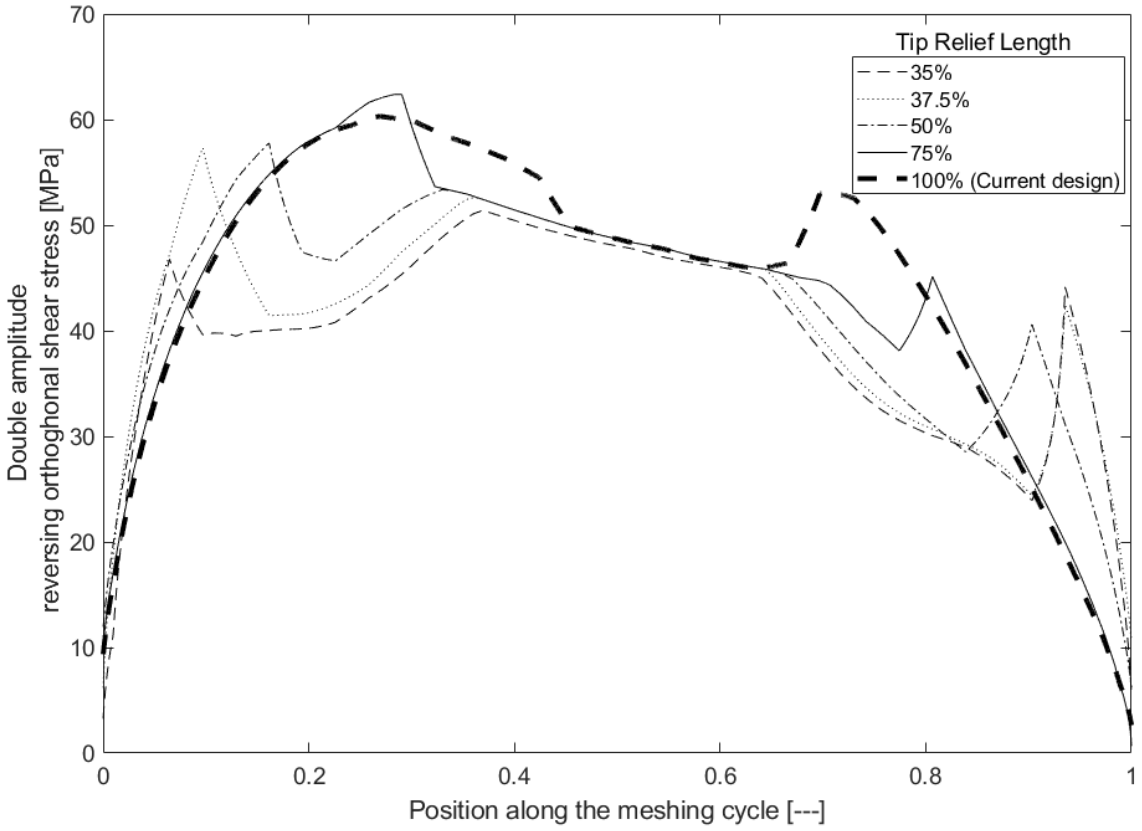

Figure 8: Double amplitude reversing orthogonal shear stress along the meshing cycle for different tip relief length; Planet-Ring Contact

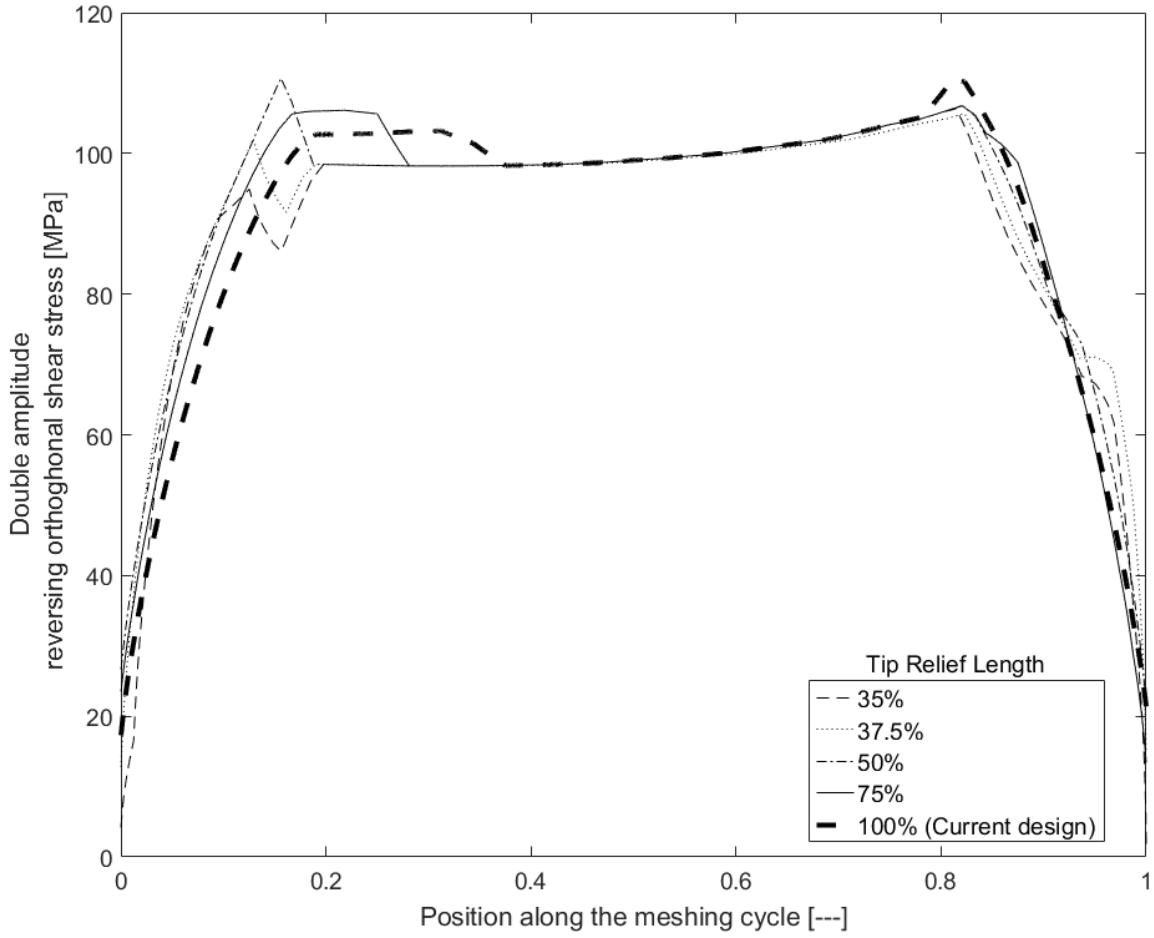

Figure 9: Double amplitude reversing orthogonal shear stress along the meshing cycle for different amounts of tip relief length; Sun-Planet Contact

The results in Figures 8 and 9 show that the equivalent stress remains below the critical limit of 235 MPa for both the Planet-Ring and the Sun-Planet contacts. By increasing the tip relief length, the effect of alternating shear stresses becomes more pronounced. These results suggest that the baseline design has the potential of improvement from a durability view-point. Again, it should be noted that the limiting

sub-surface stress levels should be used in a trade-off with the efficiency and other performance measures such as the root stresses and scuffing-scratching as well as NVH refinement.

5- Conclusions

The study investigates the effect of tip relief (length and amount) modifications on the durability of planetary wheel hub gears of off-highway vehicles.

The following conclusions are made:

I. In general the generated contact pressures are higher in Sun-Planet contact. Therefore, the maximum equivalent stress in the Sun-Planet contact is higher than that for the Planet-Ring contact.

II. In terms of tip relief modification, increasing both the amount of tip relief and its length leads to an increase in sub-surface shear stresses in mid-meshing cycle. Applying tip relief increases the duration of single contact time along the meshing cycle with the highest applied load and generated contact pressure.

III. By increasing the tip relief length, the effect of alternating shear stresses becomes more pronounced.

IV. The presented sub-surface stress field should be in a trade-off with other performance and structural integrity measures such as root stresses, as well as transmission efficiency and NVH.

6- References

[1]- Talbot, D.C., Kahraman, A. and Singh, A., “An experimental investigation of the efficiency of planetary gear sets”, Trans. ASME, J. Mechanical Design, 134(2), 2012: 021.

[2]- Marques, P.M., Camacho, R., Martins, R.C. and Seabra, J.H., “Efficiency of a planetary multiplier gearbox: Influence of operating conditions and gear oil formulation”, Tribology International, 2015, 92: 272-280.

[3]- Mohammadpour, M., Theodossiades, S. and Rahnejat, H., “Dynamics and efficiency of planetary gear sets for hybrid powertrains”, Proc. IMechE, Part C: J. Mechanical Engineering Science, 2016, 230(7-8), pp. 1359-1368.

[4]- Fatourehchi E, Mohammadpour M, King PD, Rahnejat H, Trimmer G, Williams A., “Microgeometrical tooth profile modification influencing efficiency of planetary hub gears”, International Journal of Powertrains, 2018;7(1-3):162-79.

[5]- Lundberg, G. and Palmgren, A., “Dynamic capacity of rolling bearings”, Trans. ASME, J. Applied Mechanics, 1949, 16(2), pp. 165-72.

[6]- Johns-Rahnejat, P.M. and Gohar, R., “Point contact elastohydrodynamic pressure distribution and sub-surface stress field”, In Tri-Annual Conference on Multi-Body Dynamics: Monitoring and Simulation Techniques, 1997.

[7]- Teodorescu, M., Kushwaha, M., Rahnejat, H. and Rothberg, S.J., “Multi-physics analysis of valve train systems: from system level to microscale interactions”, Proc. IMechE, Part K: J. Multi-body Dynamics, 2007, 221(3), pp. 349-361.

[8]- Li, S., Kahraman, A. and Klein, M., “A fatigue model for spur gear contacts operating under mixed elastohydrodynamic lubrication conditions”, Trans. ASME, J. Mechanical Design, 2012, 134(4): 041007.

[9]- Fatourehchi, E., Elisaus, V., Mohammadpour, M., Theodossiades, S. and Rahnejat, H., “Efficiency and durability predictions of high performance racing transmissions”, SAE Int., J. Passenger Cars-Mechanical Systems, 2016, 9(2016-01-1852).

[10]- Jao, T.C., Henly, T., Carlson, G.W., Ved, C., Carter, R.O., Hildebrand, D.H. and Ogorek, W., “Planetary Gear Fatigue Behavior in Automatic Transmission”, SAE Technical Paper, 2006.

[11]- Dong, W., Xing, Y., Moan, T. and Gao, Z., "Time domain-based gear contact fatigue analysis of a wind turbine drivetrain under dynamic conditions", Int. J. Fatigue, 2013, 48, pp. 133-146.

[12]- Bahk, C.J. and Parker, R.G., "Analytical investigation of tooth profile modification effects on planetary gear dynamics", Mechanism and Machine theory, 2013, 70, pp. 298-319.

[13] Ligata H, Kahraman A, Singh A., "An experimental study of the influence of manufacturing errors on the planetary gear stresses and planet load sharing", Journal of Mechanical Design. 2008 Apr 1;130(4):041701.

[14] Fatourehchi E, Mohammadpour M, King PD, Rahnejat H, Trimmer G, Williams A, Womersley R., "Effect of mesh phasing on the transmission efficiency and dynamic performance of wheel hub planetary gear sets", Proceedings of the Institution of Mechanical Engineers, Part C: Journal of Mechanical Engineering Science. 2017:0954406217737327.

[15]- Vijayakar, S., "CALYX manual", Advanced Numerical Solutions Inc, Columbus, Ohio, USA, 2000.

[16]- Xu, H. and Kahraman, A., "Prediction of friction-related power losses of hypoid gear pairs", Proc. IMechE, Part K: J. Multi-body Dynamics, 2007, 221(3), pp. 387-400.

[17]- Karagiannis, I., Theodossiades, S. and Rahnejat, H., "On the dynamics of lubricated hypoid gears", Mechanism and Machine Theory, 2012, 8, pp. 94-120.

[18]- Johnson, K. L., "Contact Mechanics", Cambridge university press, Cambridge, UK, 1985.

[19]- Johns-Rahnejat, P.M., "Pressure and stress distribution under elastohydrodynamic point contacts", PhD thesis, Imperial College, London, 1988

[20]- Gohar, R. and Rahnejat, H., "Fundamentals of Tribology", Imperial College Press, London, 2008.

[21]- Evans, C.R. and Johnson, K.L., "Regimes of traction in elastohydrodynamic lubrication," Proc. IMechE, Part C: J. Mechanical Engineering Science, 1986, 200(5), pp. 313–324.

[22]- Chittenden, R. J., Dowson, D., Dunn, J. F. and Taylor, C. M., "A theoretical analysis of the isothermal elastohydrodynamic lubrication of concentrated contacts. II. General Case, with lubricant entrainment along either principal axis of the Hertzian contact ellipse or at some intermediate angle", Proc. Roy. Soc., Ser. A, 1985, 397, pp. 271-294.

[23] Greenwood, J. A. and Tripp J. H., "The contact of two nominally flat rough surfaces", Proc IMechE, 1970, 185, pp. 625–633.

[24] Teodorescu, M., Balakrishnan, S. and Rahnejat, H., "Integrated tribological analysis within a multi-physics approach to system dynamics", Tribology and Interface Engineering series, 2005, 48, pp. 725-737.

[25] Mohammadpour, M., Theodossiades, S. and Rahnejat, H., "Transient mixed non-Newtonian thermo-elastohydrodynamics of vehicle differential hypoid gears with starved partial counter-flow inlet boundary", Proc. IMechE, Part J: J. Engineering Tribology, 2014, 228(10), pp. 1159-1173.

[26] Vijayakar SM. Edge effects in gear tooth contact. In: Proc. of the 7th International Power Transmission and Gearing Conference 1996 (Vol. 88, pp. 205-212).

Nomenclature

A	Apparent contact area
c'	Specific heat capacity of the solid surfaces
E_r	Reduced elastic modulus of the contact
E'	Reduced elastic modulus of the contact: $(2E_r)/\pi$
EHL	Elastohydrodynamic Lubrication
f_v	Viscous friction
h^*_{c0}	Dimensionless central lubricant film thickness
h_{c0}	Central lubricant film thickness
K	Lubricant's thermal conductivity
K'	Thermal conductivity of the solids
$\bar{p}$	Average (Laplace) contact pressure
P_m	Mean pressure
q	Traction

R	Effective radii of curvature
R_x	Radii of curvature along the direction of sliding
R_y	Radii of curvature along the direction of side leakage
TCA	Tooth Contact Analysis
U_r	Rolling velocity
U_s	Sliding velocity
U	Speed of entraining motion
α	Pressure viscosity coefficient
β	Average asperity tip radius
η_0	Lubricant dynamic viscosity at atmospheric pressure
μ	Coefficient of friction
$\boldsymbol{\rho}'$	Density of solids
τ_0	Eyring shear stress

Response to the Reviewers:

We are very grateful for the thorough and diligent review of our paper by our learned colleagues. We have strived to implement all their recommendations. We hope that the revised version of the paper and our point-by-point responses below meet with our reviewing colleagues' approval. We believe that as the result of their observations/suggestions the quality of our paper has significantly improved.

All the changes made in the revised version of the paper are highlighted for ease of monitoring by our colleagues. We have also thoroughly and carefully read through and improved the paper's grammar and punctuations. Below, we have addressed all the points raised by them individually.

Reviewer A:

Reviewer's comment: The authors present a planetary speed reducer for automotive applications on which they deal with subsurface Mode II cracks responsible for causing pitting. They calculate their loads using TCA along the path of contact and take into account boundary and EHL models to calculate stresses in the contact area.

The work is of acceptable quality and it is recommended for publishing in IJPT provided that the following points are answered and corrected:

The level of English is good in general, however a thorough search for typographical and grammatical errors should be made (i.e. 'minimize' and 'minimise' appear in the same paragraph, 'toth contact analysus' instead of 'tooth contact analysis', 'teeth pair' instead of 'tooth pair' etc.)

Our response:

We are thankful for our colleague's valuable review and constructive comments. Thank you also for observing these anomalies. These are now corrected.

Reviewer's comment: The graphs showing the characteristics of meshing (i.e. radius of curvature, rolling velocity and nominal load on teeth etc.) are plotted against the 'position along the meshing cycle' (0 to 1). The authors should clarify if this refers to % angular position or to % distance covered on the path of contact. If so, in both cases the path of contact becomes longer if tip-relief is applied, therefore

the positions of the HPSTC and LPSTC should also move with increasing tip-relief, which is not observed in the relative plots.

Our response:

We thank our colleague's valuable comment. The term 'position along the meshing cycle' refers to angular position on the path of contact. Considering different scenarios listed in Tables 2 and 3, the effect of variation of tip relief amount and tip relief length on the length of line of action is negligible. Therefore, we made the different characteristics of meshing into non-dimensional form between 0 to 1 where "0" refers to the angular position at the start of meshing and "1" refers to angular position at the end of the meshing cycle. This is now explained before section 4.1.

Reviewer's comment: Involute and tip-modified involute are smooth curves with also smooth radius of curvature along their length. Clearly the graphs illustrate non-smooth radius of curvature along the path of contact, which is obviously attributed to discretisation and numerical errors during its calculation (see particularly the last descending part of Fig. 4 upper left diagram from the HPSTC to end). Authors should revise or explain in text accordingly.

Our response:

We are thankful to our colleague for this important observation. The finite element-based TCA model which we used in this paper does not use involute equations to represent the tooth surface geometry. Instead, it uses actual coordinate information created by a simulation of the cutting process [1]. This is now explained after Figure 4.

Reviewer's comment: EHL pressure spikes are not present in Fig. 2, despite the fact that the authors mentioned them in the introduction and deemed the increase in stress caused by them as serious and potetntially detrimental. Instead they speak in general about 'viscous' friction, citing the relevant work by Johnson [16]. However, they refer to the Stribeck curve and take into account also the boundary friction domain, so it is natural that as the Stribeck number increases either due to lighter load and/or higher sliding velocity that EHL conditions should appear. Authors should comment on that.

Our response:

Our colleague is quite right. We should have explained the developed EHL model in more detail. The proposed analytical model is based on different validated models [2-4]. Moreover, the presented analytical model is time-efficient, simulating a meshing cycle of spur gear pair in a couple of seconds. This is necessary in performing a parametric study of effect of gear tip relief modification upon planetary hub sub-surface stresses. The developed analytical model calculates the contact pressure, based on the classical Hertzian theory which neglects the EHL pressure spikes. This is now explained after Figure 2.

Reviewer's comment: The TCA models used by the authors do not take into account multiple contacts of one gear, i.e. contact of the planet with the sun and the ring at two diametrical points. It is this reviewer's opinion that the combined effect of both simultaneous contacts is not taken into account concerning the distribution of loads. Authors should comment on this and clarify.

Our response:

Our colleague has raised an important point. The distribution of loads on different planet gear meshes are indeed affected by multiple simultaneous contacts. However, the trend of load distribution and consequently orthogonal shear stress for different tip relief amount and tip relief length would be the same by taking into account multiple contacts of planet gear. Therefore, for simplicity of the TCA model we neglected this effect and developed separate models for sun-planet and planet-ring contacts.

Reviewer's comment: Although the gears in question have light loads acting on them (judging from the shear stresses at contact points) and move at speeds of ~1000 RPM (sun) no rattling or other dynamic phenomena which are common in gear drives are discussed or shown. This reviewer run similar cases using standard TCA on commercial software and found significant loss of contact and therefore rattling along each meshing cycle. If the authors of this work performed a quasi-static analysis they should clearly point it out in the text, otherwise it is misleading.

Our response:

Thank you for noting this. We should have mentioned that we have performed a quasi-static analysis. This is now explained in section 3.

Reviewer's comment: The authors should at least discuss the effect of manufacturing errors, which are not taken into account, on the dynamical performance and overloading of the gears.

Our response:

We thank our colleague's valuable comment. The effects of manufacturing errors on planetary systems efficiency and durability is now discussed in the Introduction section. It is also clarified in section 3 that the effects of manufacturing errors are not taken into account in this study.

Reviewer's comment: The authors should clearly define the geometrical properties of the gear teeth of the planetary transmission in the text (i.e. number of teeth, module etc.)

Our response:

The geometrical properties of the studied planetary gear set are now listed in Table 3 (following Figure 3).

Reviewer B

Reviewer's comment: The article is well-written and structured. Nonetheless there is one minor things as follows:
Please use the suggested format for the article

Our response:

We are thankful to our colleague valuable review. We have tried our best to follow the recommended format by the IJPT journal.

References:

[1] Vijayakar SM. Edge effects in gear tooth contact. In: Proc. of the 7th International Power Transmission and Gearing Conference 1996 (Vol. 88, pp. 205-212).

[2] Chittenden RJ, Dowson D, Dunn JF and Taylor CM. A theoretical analysis of the isothermal elastohydrodynamic lubrication of concentrated contacts, II. General Case, with lubricant entrainment along either principal axis of the Hertzian contact ellipse or at some intermediate angle. Proc. Roy. Soc., Ser. A 1985; 397, pp. 271-294.

[3] Evans CR and Johnson KL. Regimes of traction in elastohydrodynamic lubrication. *Proc. IMechE, Part C: J. Mechanical Engineering Science* 1986; 200(5), pp. 313–324.

[4] Greenwood JA and Tripp JH. The contact of two nominally flat rough surfaces. *Proc. IMechE, Part C: J. Mechanical Engineering Science* 1970; 185, pp. 625–633.